A Mathematical Network Model of Ischemic Stroke

Undergraduate Research Thesis

Presented in Partial Fulfillment of the Requirements for graduation with *research distinction* in Neuroscience in the undergraduate college of The Ohio State University

by

Monica Sarkar

The Ohio State University

April 2017

Project Advisor: Dr. David Terman

Department of Mathematics

Table of Contents

Acknowledgements……..…3

Abstract……4

Introduction……..5

Methods……..…..……10

Research Overview.....…….....23

Purpose...……25

Results...…….26

Discussion……..33

References……..35

Acknowledgements

I would like to thank Dr. Terman for being such a generous and helpful mentor for the past two years. I have had the pleasure to learn about the fields of mathematical neuroscience, programming and research from you. You have always encouraged me to push myself, whether by writing a thesis or presenting at national and local conferences. I don't think I would have achieved my dream of getting into medical school without you, and now with your support, I hope to also continue performing research. It has been an honor to work in your lab and to get to know you.

To Cameron, thanks so much for going out of your way to help me with this thesis. I don't think I could have completed it without all your expertise in C and Matlab. I have enjoyed working with you for the last two years. Good luck on your future endeavors.

To Dr. Coutellier, thanks again for agreeing to be on my thesis defense committee.

To my family, thank you all very much for pushing me to finish this thesis. I'm ever grateful for your support.

Abstract

Stroke is a major cause of morbidity and mortality in the United States, with one stoke occurring every forty seconds. About eighty-seven percent of all stokes are ischemic, in which a blood vessel to the brain is blocked, resulting in an energy crisis and subsequent disruption of ion gradients. As a result, waves of recurrent spreading depolarizations (RSDs) start to spread throughout the penumbra. Eventually, extracellular glutamate builds up and leads to excitotoxicity, swelling and death of brain cells. The purpose of this research is to better understand the dynamics of the RSDs that have been associated with glutamate accumulation and growth of brain lesions. We have constructed a functioning model of 25 astrocytes and 25 neurons that incorporates membrane potentials, ion currents, cell receptors, sodium-potassium pumps and glial sodium-glutamate transporters. The network model is then reduced to 15 neuron-astrocyte pairs, so that the effect of parameters, such as neuron Na^+-K^+ ATPase strength and astrocytic Na^+-K^+ ATPase strength, on RSDs can be determined. Gap junctions between astrocytes are also included in the reduced model to understand how the number of gap junction connections and strength of gap junction impact RSDs.

Introduction

A stroke, or "brain attack," is characterized by interrupted or reduced blood flow, resulting in damage and/or death (infarction) of brain tissue (National Center for Chronic Disease Prevention and Health Promotion [NCCDPHP], 2016). Consequences may include learning, memory and speech complications, difficulty controlling emotions, paralysis, depression, and even death (NCCDPHP, 2016). Stroke is the fifth leading cause of death, killing over 130,000 American adults every year; it is also a major cause of long-term disability (NCCDPHP, 2016). There are two major types of strokes: hemorrhagic stroke, in which a blood vessel bursts and bleeds into or around the brain, and ischemic stroke, in which a blood vessel supplying the brain is blocked (National Institutes of Health). The latter is far more common, with ischemic stroke comprising eighty-seven percent of the roughly 795,000 strokes that occur every year in the United States (Mozaffarian et al., 2015).

The most common type of ischemic stroke is a thrombotic stroke, in which a blood clot or *thrombus*, typically formed from an atherosclerotic plaque within an artery of the brain, becomes lodged within that blood vessel (National Institute of Neurological Disorders and Stroke, 2004). When a freely traveling clot, or *embolus*, originating from outside the brain, blocks a blood vessel of the brain, it is known as an embolic stroke, the less common form of ischemic stroke (American Stroke Association, 2005). Treatment for ischemic stroke include: tissue plasminogen activator (tPA), a clot-busting drug; mechanical removal of the clot; and blood thinners to prevent clot formation (American Stroke Association, 2005).

Ischemia may occur focally, in a certain brain region, or globally, throughout the brain (Rossi 2007). Ischemic strokes are typically focal rather than global; they are most commonly caused by occlusion of the middle cerebral artery (Xing 2012; Iadecola and Anrather 2011).

Focal ischemia is defined by the presence of an ischemic core, the central region of the insult, in addition to the surrounding area known as the penumbra. Within the ischemic core, the cerebral blood flow is almost completely arrested, with less than 20% of basal cerebral blood flow levels (Moskowitz 2011). Due to the restricted blood flow, oxygen and glucose cannot be delivered and oxidative phosphorylation, the main process through which adenosine triphosphate (ATP) is formed, cannot occur (Rossi 2007).

ATP stores are greatly reduced to approximately 25% of basal levels (Rossi 2007, Lipton 1999). Without ATP, energy failure occurs and ion pumps, most significantly the sodium-potassium pump (also known as the sodium-potassium ATPase), can no longer maintain the ion gradient (Iadecola and Anrather, 2011). Thus, sodium (Na^+) and calcium (Ca^{2+}) accumulate within the cytoplasm of the cell while potassium rises (K^+) extracellularly, leading to rapid cell depolarization within one to three minutes (Lipton, 1999; Iadecola and Anrather, 2011). This depolarization, known as anoxic depolarization, spreads throughout the core, leading to spine loss, cell swelling and dendritic beading; the wave of anoxic depolarization later reaches the surrounding penumbral zone (Risher, 2010) The cells never repolarize again and subsequently, organelles swell and break down, and the membrane and cell degenerate through necrotic pathways (Dirnagl et al., 1999; Iadecola and Anrather, 2011). The cells of the ischemic core die within minutes of the original insult, ensuing in irreversible damage (Xing 2012).

Similar to the ischemic core, the penumbra is damaged; however, it differs in that its cells may potentially be salvaged (Lo 2008). In the penumbra, also known as the peri-infarct zone, cerebral blood flow has fallen to below functional levels but above the threshold for cell death due to a collateral blood supply (Pietrobon and Moskowitz, 2014; Xing, 2012). The neurons of the peri-infarct zone have milder ATP deficits (now 50 – 70 % of resting levels) while unable to

fire action potentials, they can maintain their -70 mV resting potentials (Lipton 1999; Lo 2008). The penumbra retains the potential to survive within a critical time window – after prolonged ischemic stress, the neurons and glia will die within a few hours and the infarct will grow (Moskowitz 2011; Iadecola and Anrather 2011). However, when blood pressure and cerebral blood flow in the penumbra were increased, the penumbral area recovered and could again transmit action potentials (Lo 2008). While perfusion prevents further damage from being done, no clinically effective neuroprotective therapy that can salvage the penumbra has been found yet (Xing 2012).

However, more is now understood about the ischemic cascade, the series of cellular and molecular events leading to brain tissue death, since the penumbra was initially discovered and defined in 1977 (Astrup, 1977). In the first few minutes of ischemia, the sodium-potassium pumps fail and ion gradients, no longer able to be maintained, slowly change and the cells depolarize (Szatkowski and Attwell 1994; Rossi 2007; Dirnagl et al., 1999). Since the decrease in ATP within the penumbra is milder than that in the core, the drastic ionic changes that occur in the core do not happen in the peri-infarct zone (Rossi 2007). Instead, recurrent spreading depolarizations (RSDs), defined as repeating waves during which there is sustained depolarization of neurons, occur in the ischemic penumbra – these waves are also known as peri-infarct depolarizations (PIDs) or transient ischemic depolarizations (TIDs) (Dreier 2011; Rossi 2007).

The cause of recurrent spreading depolarizations is thought to be the result of elevated extracellular K^+ beyond a certain threshold (Pietrobon and Moskowitz 2014; Busch et al., 1996). In the hours or days after the initial insult, recurrent peri-infarct depolarizations enlarge the size of the infarct of the core (Back et al., 1996; Busch et al., 1996; Shin et al., 2005; Nakamura et al.,

2010). The duration and frequency of these peri-infarct depolarizations correspond to how much the infarct has matured and expanded (Pietrobon and Moskowitz 2014). Spreading depolarizations typically travel through brain tissue at a speed of 2 – 6 mm/minute (Lauritzen, 1994). For some period, the neurons retain the potential to survive while under metabolic stress due to the increased need for energy to restore ion gradients (Iadecola, 2011).

A rise in glutamate in the extracellular space is associated with the degradation of ionic gradients as well as recurrent spreading depolarizations (Phillis, 1996; Higuchi 2002). Glutamate, the major excitatory neurotransmitter, accumulates extracellularly to large concentrations of 100 – 300 μM, as its release from cells is increased and its reuptake inhibited (Choi and Rothman, 1990; Xing, 2012; Iadecola, 2011). Elevated extracellular glutamate leads to cell death in a process named *excitotoxicity* (Lo 2005; Rossi 2007). Glutamate activates both metabotropic glutamate receptors and ionotropic glutamate receptors, such as the *N*-Methyl-D-aspartate (NMDA) receptor and the α-amino-3-hydroxy-5-methyl-4-isoxazolepropionic acid (AMPA) receptor (Hossmann, 1994; Moskowitz 2011). This results in calcium overload within the neurons and astrocytes (Xing 2012; Dirnagl et al., 1999; Rossi 2007). Through over-activation of the glutamate receptors, there is also a massive influx of Na^+ and Cl^-, followed by water to maintain osmotic equilibrium, leading to cell swelling or edema; K^+ exits the cell (Dirnagl et al., 1999). The ion gradients of the cells are further decreased and more ATP is consumed, which leads to more glutamate being released (Rossi 2007).

The calcium overload activates calcium-dependent synthases and proteases that degrade vital cell proteins (Moskowitz, 2011; Lo, 2005). Additionally, the mitochondria begin to fail and can no longer perform oxidative phosphorylation (Ankarcrona, 1995; Lo, 2005). Reactive oxygen species (ROS) are released and attack cell proteins, lipids and nucleic acids, further

breaking the cell (Lipton 1999; Lo 2005). Brain cells finally die either through apoptosis and necrosis (Ankarkrona 2005; Lo 2005).

The main source of glutamate release has been found to be the reversal of the glutamate transporters (Rossi 2000; Rossi 2007). Under normal, non-ischemic conditions, the transporter uptakes 1 proton, 3 Na^+ and 1 glutamate for every 1 K^+ that is released into the extracellular space (Levy, 1998). Under ischemic conditions, however, the ion gradients are dissipated and the Na^+-glutamate transporter reverses and releases glutamate extracellularly. Na^+–glutamate transporters are present in both neurons and astrocytes, having a far higher density in the latter (Rossi 2007). Neuronal transporters, having a higher concentration of intracellular glutamate, are more likely to reverse than their glial counterparts (Rossi 2007). Some studies suggest neurons release glutamate while astrocytes take it in during ischemia (Rossi 2007). This is supported by findings from recent studies that imply the Na+-glutamate transporter in astrocytes, EAAT2, is responsible for most brain glutamate uptake (Danbolt 2016).

Gap junctions are clusters of channels between cells that allow for diffusion of ions and molecules such as Na^+ and K^+ when open (Farahani 2005). There is currently debate about the role of astrocyte gap junctions may play in spreading depolarizations. Prior to the start of spreading depolarizations, astrocytes serve to prevent them by taking in extracellular glutamate and K^+ through gap junctions (Farahani 2005, Somjen 2001). However, after the initiation of spreading depolarizations, glia may help propagate waves further by spreading K^+ through its gap junctions (Somjen 2001). Additionally, some studies suggest that apoptotic and necrotic signals may be transmitted by glial gap junctions (Farahani 2005).

Methods

Equations

The model consists of a total of twenty-five astrocytes and twenty-five neurons. Both cell types include equations simulating cell membrane potentials, ion currents and fluxes through channels, pumps and transporters, as well as the membrane and ion dynamics of the extracellular space. Neurons and astrocytes are both modeled as single-cell compartments, as per Hodgkin-Huxley formalism (Source)

Neuron

The change in the resting potential, *V*, of each neuron is modeled here, as per the Goldman-Hodgkin-Katz equation (Ermentrout 2010).

$$C\frac{m dV}{dt} = -I_{Na} - I_{NaP} - I_K - I_L - I_{pump} - I_{NMDA} - I_{Ca,pump} \quad (1)$$

The terms of the right-hand side represent the fast sodium, persistent sodium, potassium, leak, sodium-potassium pump, sodium-glutamate transporter and calcium pump currents, respectively.

Let:

$$\varphi = \frac{F}{RT}\, V\,, \quad (2)$$

where *R*, *T* and *F* are the gas constant, absolute temperature (in kelvin) and Faraday's constant respectively.

The I_{Na}, I_{NaP} and I_K currents are given below:

$$I_{Na} = P_{Na}\, m_\infty^3(V)\, h\, F\, \varphi\, \frac{([Na^+]_e\, e^{-\varphi} - [Na^+]_i)}{(\, e^{-\varphi} - 1)} \quad (3)$$

$$I_{NaP} = P_{NaP}\, m_{p\infty}(V)\, h_p\, F\, \varphi\, \frac{([Na^+]_e\, e^{-\varphi} - [Na^+]_i)}{(\, e^{-\varphi} - 1)} \tag{4}$$

$$I_K = P_K\, n^4\, F\, \varphi\, \frac{([K^+]_e\, e^{-\varphi} - [K^+]_i)}{(\, e^{-\varphi} - 1)} \tag{5}$$

P_{Na}, P_{NaP} and P_K are the permeability constants for each ion. $[Na^+]_e$ and $[K^+]_e$ represent the extracellular concentrations of Na^+ and K^+, respectively. $[Na^+]_i$ and $[K^+]_i$ are the intracellular concentrations of Na^+ and K^+, respectively.

n^4 represents the probability that the K^+ channel is open (Ermentrout 2010). $m_\infty^3(V)$ and $m_{p\infty}(V)$ represent the probability that the transient and persistent sodium activation gates are open, respectively. h and h_p corresponds to the probability that the transient and persistent sodium inactivation gates are open. $h = 1 - n$, as per the Rinzel reduction of the Hodgkin-Huxley equations (Ermentrout 2010; Huguet 2016).

The variables h_p and n satisfy the following equation, where X = h_p and n:

$$\frac{dX}{dt} = \phi_X\, \frac{X_\infty(V) - X}{\tau_X(V)}\,, \tag{6}$$

Where = ϕ_n = 0.8 and ϕ_h = 0.05, V_n = -34.

The function $X_\infty(V)$ is of the form below:

$$X_\infty(V) = \frac{1}{1 + e^{-\frac{V - V_X}{\sigma_X}}} \tag{7}$$

The time constant functions, τ_n and τ_{hp}, are of the form below.

$$\tau_n(V) = 0.05 + \frac{0.27}{1 + e^{\frac{V+40}{12}}} \quad and \quad \tau_{h_p}(V) = \frac{10000}{cosh\left(\frac{V+49}{12}\right)} \tag{8}$$

The values of the parameters are as follows: $V_m = -34,\ \tau_m = 5,\ V_n = -55,\ \tau_n = 14,$

$$V_{m_p} = -40,\ \tau_{m_p} = 6,\ V_{h_p} = -48,\ \tau_{h_P} = -6$$

The current of the leak channel satisfies the following equation:

$$I_L = g_L\,(V - E_L) \tag{9}$$

where the g_L represents the membrane conductance of the leak channel, whereas E_L is the Nernst or reversal potential for the leak channel.

The current of the sodium-potassium pump (from Kager 2000)

$$I_{pump} = \rho_N \left(\frac{[K^+]_e}{K_{K,N} + [K^+]_e}\right)^2 \left(\frac{[Na^+]_i}{K_{Na,N} + [Na^+]_i}\right)^3 \tag{10}$$

$K_{K,N}$ corresponds to the half activation [K+] concentration, and $K_{Na,N}$ to the half activation [Na+] concentration of the neuronal Na+-K+ ATPase.

The total current of the NMDA channel is the sum of the Na^+, K^+ and Ca^{2+} currents traveling through the receptor, as given below:

$$I_{NMDA} = I_{NMDA}^{Na} + I_{NMDA}^{K} + I_{NMDA}^{Ca} \tag{11}$$

The current due to each ion specie is as follows.

Na^+ NMDA current:

$$I_{NMDA}^{Na} = P_{NMDA}\, s_G\, b_\infty(V_N)\, F\, \varphi\, \frac{([Na^+]_e\, e^{-\varphi} - [Na^+]_i)}{(\, e^{-\varphi} - 1)} \tag{11}$$

K^+ NMDA current:

$$I_{NMDA}^{K} = P_{NMDA}\, s_G\, b_\infty(V)\, F\, \varphi\, \frac{([K^+]_e\, e^{-\varphi} - [K^+]_i)}{(\, e^{-\varphi} - 1)} \tag{12}$$

Ca^{2+} NMDA current:

$$I_{NMDA}^{Ca} = 2\, P_{Ca}\, P_{NMDA}\, s_G\, b_\infty(V)\, F\, \varphi\, \frac{([Ca^{2+}]_e\, e^{-\varphi} - [Ca^{2+}]_i)}{(\, e^{-\varphi} - 1)} \tag{13}$$

P_{NMDA} is the NMDA channel permeability constant; $P_{Ca} = 3$. $[Ca^{2+}]_e$ and $[Gl]_e$ represent the extracellular concentrations of Ca^{2+} and glutamate respectively. $[Ca^{2+}]_i$ and $[Gl]_i$ are the intracellular concentrations of Ca^{2+} and glutamate, respectively. The function $b_\infty(V)$ is of the form (7), with $V_b = -10$ and $\sigma_B = 16.13$.

s_G is the NMDA channel state variable, for which the equation is given below:

$$\frac{ds_G}{dt} = \left(-\frac{s_G}{t_{decay}} + \alpha_N\, s_\infty([Gl]_e)(1 - s_G) \right) \tag{14}$$

$s_\infty([Gl]_e)$ is of the form (7) with $V_s = 0.01$ and $\sigma_s = 0.001$; $\alpha_N = 0.5$ and $t_{decay} = 1$.

The calcium current through the calcium pump, which extrudes calcium from the cell, is given:

$$I_{Ca,pump} = \rho \frac{[Ca^{2+}]_i}{K_{cap} + [Ca^{2+}]_i} \tag{16}$$

in which $\rho = 0.5$ and $K_{cap} = 0.3$.

All parameter values for the neuron are given in Table 1.

Astrocyte

Below is the differential equation which models how the resting potential of an astrocyte, V_A, changes over time. The right-hand terms represent the sodium, potassium, Na+-K+ pump, Na+-glutamate transporter and gap junction currents in the astrocyte, respectively.

$$C_m^A \frac{dV_A}{dt} = -I_{Na}^A - I_K^A - I_{pump}^A - I_{NaGl}^A - I_{gap} \tag{17}$$

Here, the K^+, Na^+ and Na^+-K^+ ATPase currents are given:

$$I_K^A = P_K^A \; F \; \varphi_A \frac{[K^+]_e \, e^{-\varphi A} - [K^+]_{iA}}{e^{-\varphi A} - 1} \tag{18}$$

$$I_{Na}^A = P_{Na}^A \; F \; \varphi_A \frac{[Na^+]_e \, e^{-\varphi A} - [Na^+]_{iA}}{e^{-\varphi A} - 1} \tag{19}$$

$$I_{pump}^A = \rho_A \left(\frac{[K^+]_e}{K_{K,A} + [K^+]_e} \right)^2 \left(\frac{[Na^+]_{iA}}{K_{Na,A} + [Na^+]_{iA}} \right)^3 \tag{20}$$

As in (10), $K_{K,A}$ corresponds to the half activation [K+] concentration, and $K_{Na,A}$ to the half activation [Na+] concentration of the neuronal Na+-K+ ATPase.

The φ_A function is the same as that in (5) – the voltage of the astrocyte, V_A, is substituted in place of the voltage of the neuron, V.

Below, the reversal potential of the Na+-glutamate transporter in the astrocyte is given:

$$E_{NaGl}^A = \frac{RT}{2F} \ln \left\{ \left(\frac{[Na^+]_e}{[Na^+]_{iA}} \right)^3 \left(\frac{[K^+]_{iA}}{[K^+]_e} \right) \left(\frac{[Gl]_e}{[Gl]_{iA}} \right) \left(\frac{[H^+]_e}{[H^+]_{iA}} \right) \right\} \tag{21}$$

$[Gl]_{iA}$ is the intracellular glutamate concentration of the astrocyte. $[H^+]_e$ and $[H^+]_{iA}$ are the proton concentrations outside and within the astrocyte, respectively. The quantity of ($[H^+]_e$ / $[H^+]_{iA}$) is assumed to be at a constant value of 0.5 (Rossi 2000)

The current of the astrocytic Na+-glutamate transporter is given as:

$$I_{NaGl}^{A} = g_{NaGl}^{A} \left(V_A - E_{NaGl}^{A}\right) \tag{22}$$

where g_{NaGl}^{A}l is the conductance of the transporter. Under physiological conditions, $I_{NaGl}^{A} > 0$, but under ischemic conditions, the transporter reverses and $I_{NaGl}^{A} < 0$.

Gap junctions are also modeled, as per the Goldman-Hodgkin-Katz equation. The voltage difference between astrocytes *j* and *k*, $V_A^j - V_A^k$, is the driving force of currents due to gap junctions (Huguet 2016)

$$\phi^{jk} = \frac{F}{RT}\left(V_A^j - V_A^k\right) \tag{23}$$

The K^+ and Na^+ currents flowing through the gap junction between astrocytes *j* and *k* are given below:

$$I_{K,gap}^{jk} = P_{K,gap}\, F\, \phi_{gap}^{jk} \left(\frac{[K^+]_i^k\, e^{-\phi^{jk}} - [K^+]_{i,A}^j}{e^{-\phi^{jk}} - 1}\right) \tag{24}$$

$$I_{Na,gap}^{jk} = P_{Na,gap}\, F\, \varphi_{gap}^{jk} \left(\frac{[Na^+]_i^k\, e^{-\phi^{jk}} - [Na^+]_{i,A}^j}{e^{-\phi^{jk}} - 1}\right) \tag{25}$$

The permeability of the K^+ and Na^+ gap junctions, $P_{K,gap}$ and $P_{Na,gap}$, respectively, are as follows, where σ_{gap} is a parameter that determines the strength of the gap junction and is tested at different values.

$$P_{K,gap} = \sigma_{gap} P_K \quad \text{and} \quad P_{Na,gap} = 0.8\, P_{K,gap} \tag{26}$$

Astrocytes may have multiple gap junctions with other cells; thus, the total K^+ current due to gap junctions for astrocyte *j* is the sum of the potassium currents flowing through all the gap junctions between astrocyte *j* and other cells. The same holds for Na^+ currents.

$$I^j_{K,gap} = \sum I^{jk}_{K,gap} \qquad and \qquad I^j_{Na,gap} = \sum I^{jk}_{Na,gap} \tag{27}$$

For astrocyte j, the total current due to gap junctions is the sum of the total Na^+ and total K^+ currents, as follows.

$$I^j_{gap} = I^j_{K,gap} + I^j_{Na,gap} \tag{28}$$

All parameter values for the astrocyte are given in Table 1.

Ion concentrations

The change in extracellular K+ is modeled by the following equation:

$$\frac{\partial [K^+]_e}{\partial t} = D_K \frac{\partial^2 [K^+]_e}{\partial x^2} + \frac{10 S_N}{F \Omega_E} \left(I_K + I^K_{NMDA} - 2 I_{pump} \right) + \frac{10 S_A}{F \Omega_E} \left(I^A_K - I^A_{NaGl} - 2 I^A_{pump} \right) + D_{KR} ([K^+]_R - [K^+]_e) \tag{29}$$

The first term on the right-hand side, $D_K \frac{\partial^2 [K^+]_e}{\partial x^2}$, corresponds to the diffusion of K^+ in the extracellular space and D_K = 0.002 ms^{-1}. S_N refers to the surface area of the neuron. Ω_E is the

volume of the extracellular space, which is 2% of the neuronal volume. $[K^+]_R$ is the concentration of K^+ in the K^+ reservoir surrounding the cells and D_{KR} = 3 x 10^{-5} ms^{-1}.

The equation for extracellular Na^+ levels is the same as (29), with corresponding Na+ currents substituted:

$$\frac{\partial[Na^+]_e}{\partial t} = \frac{D_{Na}\partial^2[Na^+]_e}{\partial x^2} + \frac{10S_N}{F\Omega_E}\left(I_{Na} + I_{NMDA}^{Na} + I_{NaP} + 3I_{NaGl} + 3I_{pump}\right)$$

$$+ \frac{10S_A}{F\Omega_E}\left(I_{Na}^A + 3I_{NaGl}^A + 3I_{pump}^A\right) + D_{NaR}([Na^+]_R - [Na^+]_e) \qquad (30)$$

D_{NaR}, like D_{KR}, is equal to 3 x 10^{-5} ms^{-1}, whereas D_{Na} = 0.00133 ms^{-1}.

The extracellular glutamate, dependent on the astrocytic Na^+ – glutamate transporter current as well as diffusion of glutamate in the extracellular space, is modeled:

$$\frac{d[Gl]_e}{dt} = \frac{D_G\partial^2[Gl]_e}{\partial x^2} + \frac{10S_A}{F\Omega_E}\, I_{NaGl}\,, \qquad (31)$$

where D_G = 0.001 ms^{-1} and S_A is the surface area of the astrocyte.

The K^+, Na^+ and glutamate diffusion coefficients in the extracellular fluid (not included in the equations) are given by $\overline{D}_K$ = 1.96 × 10^{-5} cm^2/s, $\overline{D}_{Na}$ = 1.33× 10^{-5} cm^2/s, and $\overline{D}_G$ = 2.03× 10^{-5} cm^2/s, (Hille, 2001). The coefficients D_K, D_{Na} and D_G are obtained from $\overline{D}_K$, $\overline{D}_{Na}$ and $\overline{D}_G$ scaled by the square of the average distance δ between neurons: δ ≈ 3.13×10−2 mm. In addition, calcium is present in the neuron alone, entering through the NMDA channel and extruded into the extracellular space by a calcium pump. The extracellular calcium equation satisfies the following equations:

$$\frac{d[Ca^{2+}]_e}{dt} = \frac{10S_N}{F\Omega_E}(I_{NMDA}^{Ca} + I_{Ca,pump}) + D_{CaR}([Ca^{2+}]_R - [Ca^{2+}]_e) \quad (32)$$

The equations of the neuron's intracellular K+ and Na+ concentrations are given as:

$$\frac{d[K^+]_i}{dt} = -\frac{10S_N}{F\Omega_N}\left(I_K + I_{NMDA}^K - 2I_{pump}\right), \quad (33)$$

$$\frac{d[Na^+]_i}{dt} = -\frac{10S_N}{F\Omega_N}\left(I_{Na} + I_{NaP} + I_{NMDA}^{Na} + 3I_{pump}\right), \quad (34)$$

where Ω_N, the volume of the neuron, is equal to 2160 μm^3.

The intracellular K^+ and Na+ concentrations within the astrocyte fulfill the following equations:

$$\frac{d[K^+]_{iA}}{dt} = -\frac{10S_N}{F\Omega_A}\left(I_K^A + I_{NaGl}^A - 2I_{pump}^A - I_{K,gap}\right), \quad (35)$$

$$\frac{d[Na^+]_{iA}}{dt} = -\frac{10S_N}{F\Omega_A}\left(I_{Na}^A + 3I_{NaGl}^A + 3I_{pump}^A - I_{Na,gap}\right), \quad (36)$$

where Ω_A, the volume of the astrocyte, equals 2000 μm^3.

Experimental Setup

Part 1 – Model a network of twenty-five neuron-astrocyte pairs, per the preceding equations to understand the dynamics of membrane potential, currents and ion concentrations in both astrocytes and neurons. The twenty-five neurons are in a one-dimensional array, as are the twenty-five astrocytes, where each neuron-astrocyte pair shares an extracellular space.

Part 2 – Using a smaller network of fifteen astrocyte-neuron pairs, let the N_{cell} be the number of astrocytes set at an astrocytic Na^+-K^+ ATPase strength of $\rho_A low$, a parameter. The rest of 15 – N_{cell} astrocytes are set at a constant ρ_A of 1, while all the neurons are set at a fixed ρ_N of 5. Different values of $\rho_A low$ are used to determine what N_{cell} is necessary for recurrent spreading depolarizations to occur. The number of gap junctions per side, G (for a total of 2G gap junctions per astrocyte) is increased from 1 to 2 to 5. Schema is shown in Figure 3.

Part 3 – Again using a network of fifteen astrocyte-neuron pairs, let the N_{cell} be the number of astrocytes set at a constant astrocytic Na^+-K^+ ATPase strength ($\rho_A low$) of 0.05. The other 15 – N_{cell} astrocytes are set at a fixed ρ_A value of 1. Here, the parameter being tested is ρ_N, the Na^+-K^+ ATPase strength for all neurons, which is decreased from 5 to 1, as well as σ_{gap}, the strength of the gap junction, increased from 0.1 to 0.3 to 0.5. The number of gap junctions per side, G (for a total of 2G gap junctions per astrocyte) is increased from 1 to 5 to determine the effect of gap junctions on waves. Schema is shown in Figure 3.

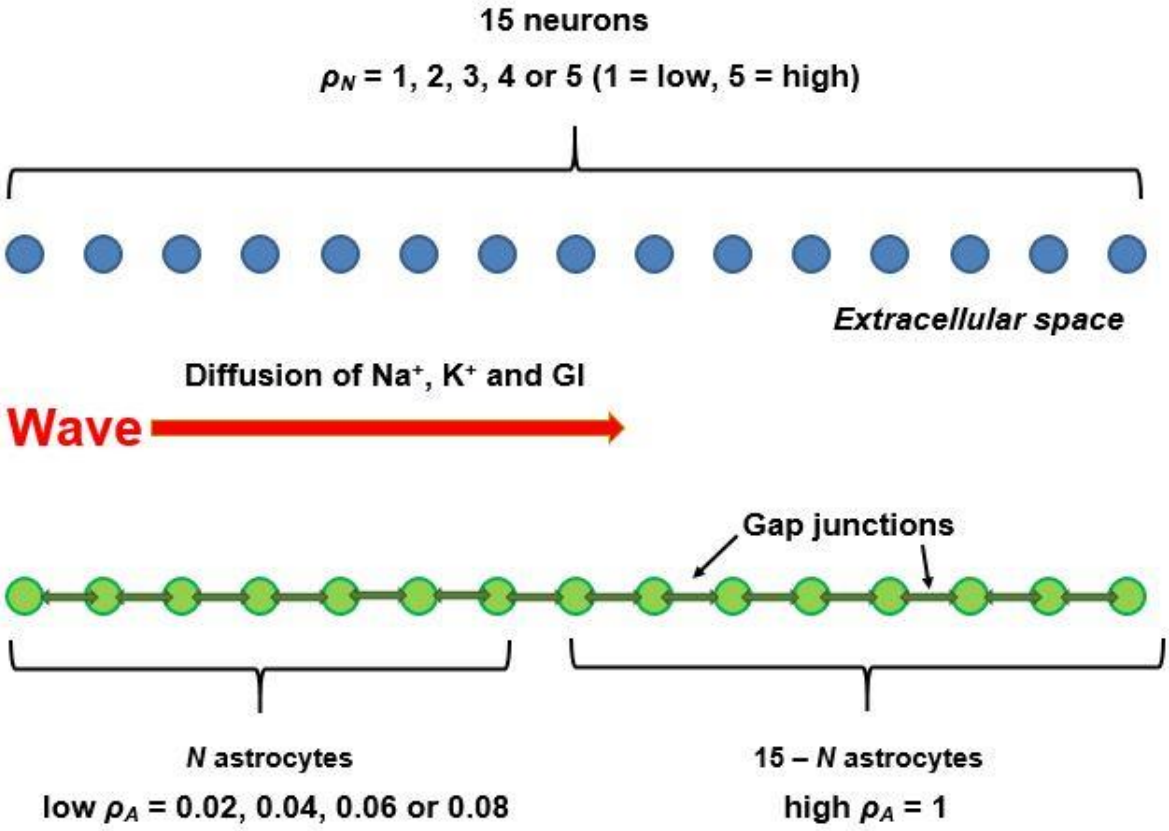

Figure 3: Schema for Parts 2 and 3

Table 1 – Neuron Parameters

Notation	Value	Unit	Description
R	8.31	J/mol K	Ideal gas constant
F	96,485	C/mol	Faraday's constant
T	310	K	Absolute temperature
S_N	922	μm^2	Surface area of neuron
Ω_N	2160	μm^3	Volume of neuron
C_m	1.00	$\mu F/cm^2$	Neuron membrane capacitance per unit area
ϕ_n	0.80	ms^{-1}	Maximum rate of activation of potassium channels
ϕ_h	0.05	ms^{-1}	Maximum rate of activation of sodium channels
P_{Na}	1×10^{-5}	cm/s	Neuron fast Na^+ permeability coefficient
P_{NaP}	3×10^{-8}	cm/s	Neuron persistent Na^+ permeability Coefficient
$[Ca^{2+}]_i$	1.3×10^{-2}	μM	Intracellular calcium concentration
P_K	7×10^{-5}	cm/s	Neuron K^+ permeability coefficient
P_{NMDA}	3×10^{-6}	cm/s	Neuron NMDA permeability coefficient
g_L	0.03	mS/cm^2	Neuron leak current conductance
E_L	-60.0	mV	Neuron leak current reversal potential
$K_{K,N}$	2	mM	Half-activation [K+] concentration for the neuronal Na^+-K^+ ATPase
$K_{Na,N}$	7.7	mM	Half-activation [Na+] concentration for the neuronal Na^+-K^+ ATPase
ρ_N	parameter	$\mu A/cm^2$	Maximum neuron Na^+-K^+ ATPase strength

Table 2 – Astrocyte Parameters

Notation	Value	Unit	Description
S_A	1600	μm^2	Surface area of astrocyte
Ω_A	2000	μm^3	Volume of astrocyte
C_m^A	1.00	$\mu F/cm^2$	Astrocyte membrane capacitance per unit area
P_{Na}^A	1.5×10^{-8}	cm/s	Astrocyte Na^+ permeability coefficient
P_K^A	4.8×10^{-6}	cm/s	Astrocyte K^+ permeability coefficient
g_{NaGl}^A	3×10^{-5}	mS/cm^2	Maximum conductance of astrocyte Na^+-glutamate transporter
σ_{gap}	parameter	unitless	Measure of gap junction strength
$K_{K,A}$	2	mM	Half-activation [K+] concentration for the astrocytic Na^+-K^+ ATPase
$K_{Na,A}$	7.7	mM	Half-activation [Na+] concentration for the astrocytic Na^+-K^+ ATPase
ρ_A	parameter	$\mu A/cm^2$	Maximum astrocyte Na^+-K^+ ATPase strength
$\rho_A low$	parameter	$\mu A/cm^2$	Maximum astrocyte Na^+-K^+ ATPase strength for N_{cell} astrocytes
N_{cell}	parameter	astrocytes	Number of astrocytes set at $\rho_A low$

Table 3 – Ion Concentration Parameters

Notation	Value	Unit	Description
D_{KR}	3×10^{-5}	ms^{-1}	Diffusion coefficient of K^+ in reservoir
D_{NaR}	3×10^{-5}	ms^{-1}	Diffusion coefficient of Na^+ in reservoir
D_{CaR}	3×10^{-5}	ms^{-1}	Diffusion coefficient of Ca^{2+} in reservoir
$[K^+]_R$	140	mM	Concentration of K^+ in reservoir
$[Na^+]_R$	10	mM	Concentration of Na^+ in reservoir
$[Ca^{2+}]_R$	3.0	μM	Concentration of Ca^{2+} in reservoir

Research Overview

Preliminary studies

Prior to studying recurrent spreading depolarizations, we created a detailed model of a single astrocyte and neuron pair, as shown in Figure 1. The core process of spreading depolarization can be modeled in a single neuron (Dreier 2011). Both the model of the neuron and that of the astrocyte included sodium currents, persistent sodium currents, potassium currents, Na^+-K^+ ATPase currents. ρA and ρN are parameters that correspond to the maximum astrocyte Na+-K+ ATPase strength and maximum neuron Na+-K+ ATPase strength, respectively.

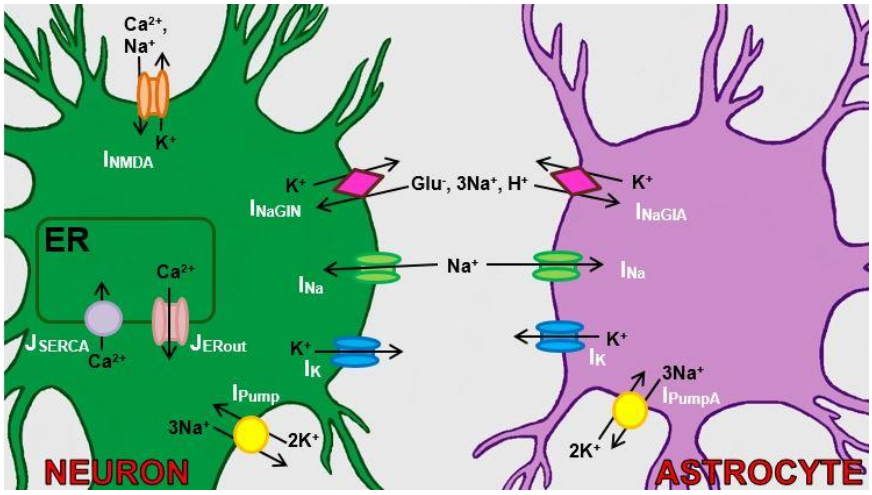

Fig. 1: Schema of model

The neuron model also included calcium (Ca^{2+}) dynamics, which followed the Rinzel-Li model (Li 1994; Fall 2001). In the neuron, there is an endoplasmic reticulum (ER) compartment that takes in or releases Ca^{2+} into the surrounding cytosol within the neuron. Additionally, there is a nearby Ca^{2+} reservoir or bath surrounding both the neuron and astrocyte. The astrocyte model incorporates the Na^+–glutamate transporter. Originally, as in Figure 1, the transporter was present in both the neuron and astrocyte. However, the neuronal Na+-glutamate transporter was

removed, as recurrent spreading depolarizations that resembled experimental results could not be attained.

In the beginning, the model is at rest with $\rho A = \rho N = 5$; slowly ρA was decreased to 0.08, a low value. The solution of the model is shown below in Figure 2. The neuronal voltage and intracellular Na^+ concentration oscillate, as well the extracellular concentrations of Na^+, K^+ and glutamate. Over time, the neuronal intracellular concentrations of K^+ and Ca^{2+}, as well as the astrocytic intracellular concentrations of Na^+, build up. Only the astrocytic intracellular concentration of K^+ decreases over time. Each depolarization lasts approximately 2 minutes; past studies have shown the duration of spreading depolarizations to be within 1.5 and 2.36 minutes (Risher, 2010; Hartings et al., 2011). The duration between depolarizations is approximately 15 minutes, which is well within the range of 5-150 minute intervals observed in humans (Nakamura et al., 2010).

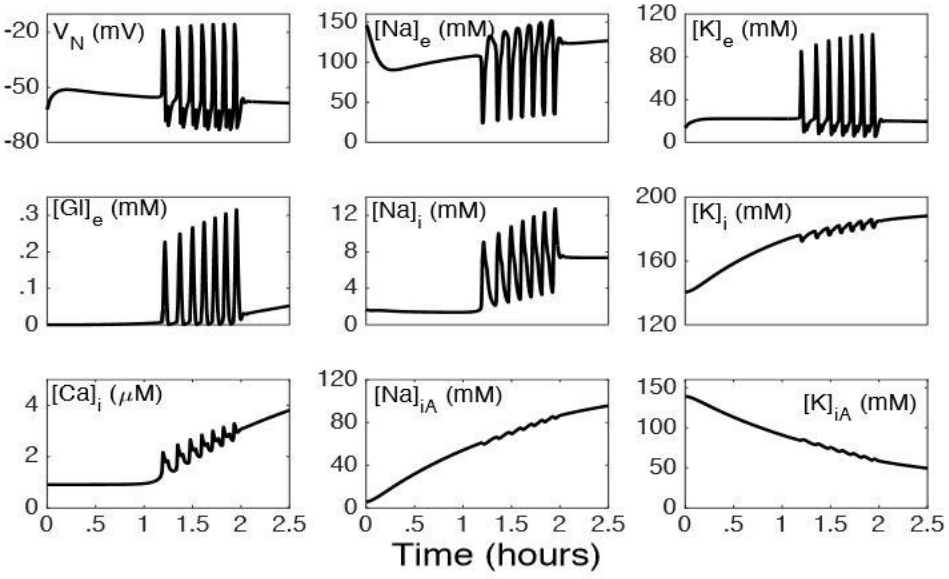

Figure 2: Solution of the model. As ρA decreases from 5 to 0.08, a total of 7 depolarizations occur within the span of roughly one hour.

Purpose

To accurately simulate the process of recurrent spreading depolarizations and understand what changes in membrane potentials and ion concentrations occur. Another goal is to understand how the astrocytic Na+-K+ ATPase strength, strength of the gap junction and number of gap junctions per astrocyte changes the number of cells necessary to induce recurrent spreading depolarizations. Our findings may also suggest possible avenues to explore in future experiments. By more fully illuminating the dynamics of ischemic stroke, better stroke medicines and therapies can be developed and improved.

Results

Part 1

There are seven episodes of spreading depolarization, as seen in Figure 4A, that occur when ρ_N= 5 and when ρ_A = 0.05 for the first five astrocytes and then increases linearly over the next 20 astrocytes such that ρ_A for the twenty-fifth and final astrocyte is equal to 2.5. As shown in Figure 4B, depolarization first occurs in the neurons opposite the astrocytes with the lowest ρ_A value of 0.05 and then spreads in a wave-like fashion to neurons that are across from astrocytes with greater ρ_A values. Thus, the twenty-fifth neuron is last to depolarize. Waves of depolarization also occurred in astrocytes in the same manner, with depolarization beginning in the astrocytes with the lowest ρ_A and reaching astrocytes with the largest ρ_A last. The waves pictured in Figure 4C travel across about one to two cells per second, from which the wave speed can be calculated. With the average distance δ between neurons ≈ 3.13×10^{-2} mm, the wave speed is approximately 2-4 mm/min, consistent with published results (Pietrobon and Moskowitz, 2014).

V_N, $[K^+]_e$ and $[Gl]_e$ are plotted when neuron 10 undergoes a depolarization. V_N and $[K^+]_e$ increase simultaneously and suddenly, while $[Gl]_e$ increases more slowly. Thus, it appears recurrent spreading depolarizations occur due to the elevation of $[K^+]_e$, rather than that of $[Gl]_e$. These results are consistent with previous findings, in which K^+ diffusion in the extracellular space is the driving factor behind spreading depolarizations, rather than glutamate diffusion (Enger, 2015).

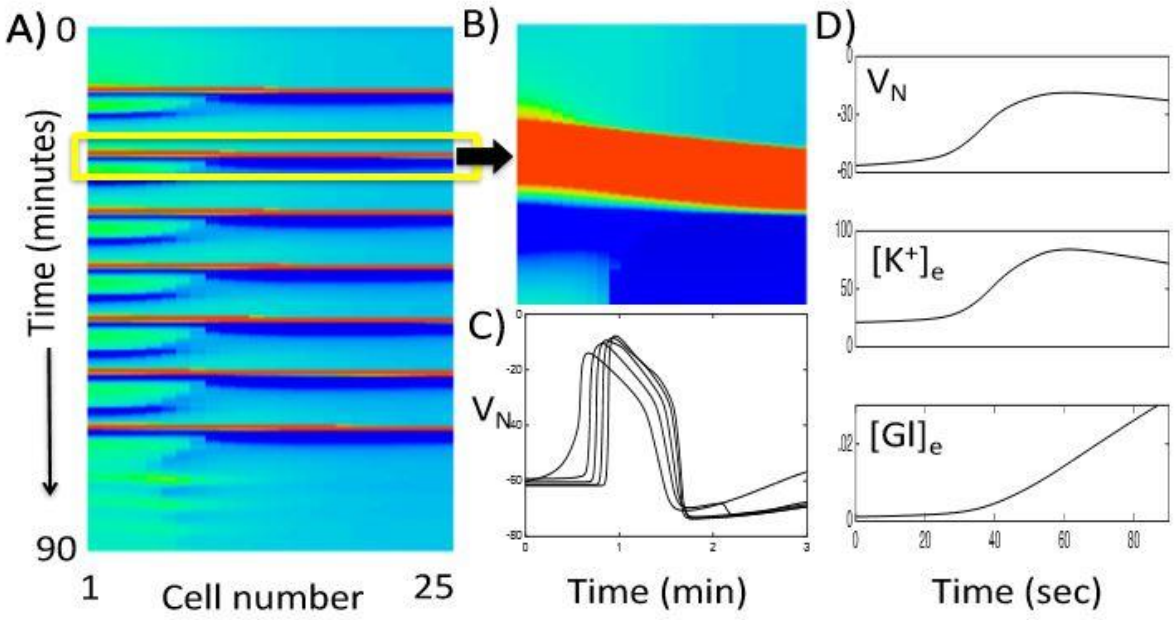

Figure 4: (A) Solution of the model with 25 neurons and 25 astrocytes. Every column represents a neuron's membrane potential over 90 minutes. ρA = .05 for the first 5 astrocytes and then increases linearly to ρA = 2.5 for astrocyte 25, while ρN = 5 for all neurons. B) A 3-minute blow-up of a depolarization episode. C) Membrane potentials of neurons 1, 10, 15, 20 and 25. D) Time courses of V_N, $[K+]_e$ and $[Gl]_e$ for neuron 10 during the second depolarization episode.

Part 2

When there were zero gap junctions, a minimum of 7 astrocytes was necessary for recurrent spreading depolarizations to occur, at all values of $\rho_A Low$ from 0.01 to 0.08 μA/cm^2 (Fig 5a). Additionally, when six astrocytes were at a $\rho_A Low$ of 0.01 μA/cm^2, spreading depolarizations occurred. When each astrocyte had 1 gap junction connection with its closest neighbor on each side (for a total of 2 gap junctions per astrocyte), waves of spreading depolarization occurred when there were at least 9 astrocytes at a $\rho_A Low$ of 0.01 μA/cm^2 (Fig 5b). Recurrent spreading depolarizations also occurred when there were 8 astrocytes at $\rho_A Low$, but only when $\rho_A Low$ ranged from 0.01 to 0.05 μA/cm^2. When every astrocyte had 5 gap junctions on each side (for a total of 10 gap junctions) a minimum of 10 astrocytes set at $\rho_A Low$ was necessary for waves to occur, with $\rho_A Low$ ranging from 0.01 to 0.08 μA/cm^2 (Figure 5c).

In summary, as the number of gap junctions per side increased from 1 to 2 to 5, higher values of N_{cell} values, or more astrocytes set at $\rho_A Low$, a low Na^+-K^+ ATPase strength, were necessary for waves of spreading depolarization to occur.

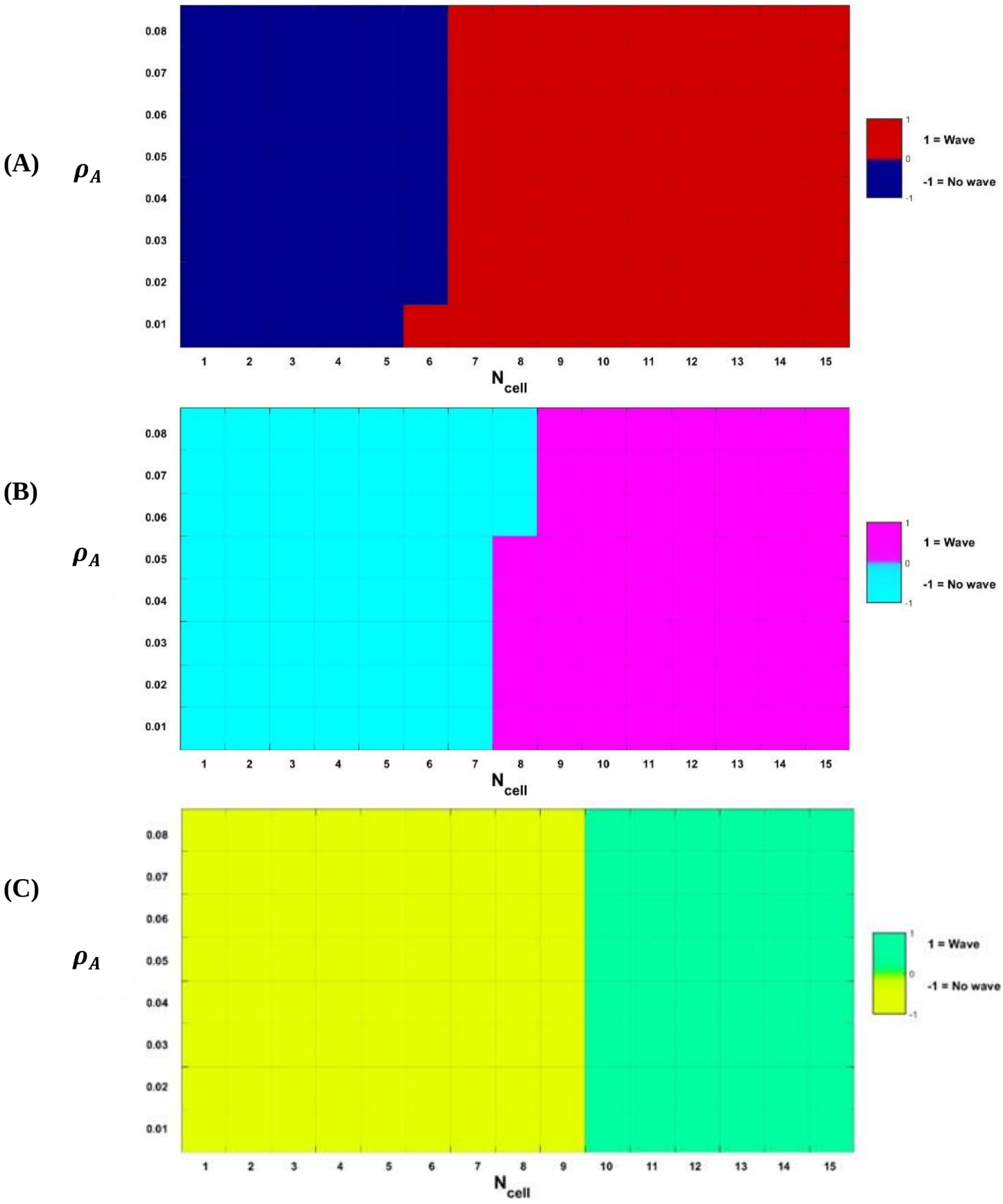

Figure 5: Presence or absence of RSDs at various ρ_A and N_{cell} values when: A) each astrocyte has 1 gap junction per side; B) when each astrocyte has 2 gap junctions per side; and C) when each astrocyte has 5 gap junctions per side.

Part 3

The effect of increasing σ_{gap} as well as ρ_N at different numbers of gap junctions was tested. A constant $\rho_A low$ of 0.05 and ρ_A of 1.00 were used.

When σ_{gap} = 0.1 (Figure 6A), as ρ_N increased from 1 to 5, the number of cells at $\rho_A low$ needed to begin recurrent spreading depolarizations increased as well, at all numbers of gap junctions per cell (Figure 3A). N_{cell}, the number of cells needed for recurrent spreading depolarizations (set at the low astrocytic Na+-K+ ATPase strength of 0.05), was greatest when there were 5 gap junctions on each side of the astrocyte. The second-highest N_{cell} values occurred when there were 3 and 4 gap junctions per side, at every value of ρ_N; N_{cell} values for 3 or 4 gap junctions per side were 2-5 less than those at 5 gap junctions/side. When there were 2 gap junctions per side, N_{cell} was the same as that for 3 and 4 gap junctions, except at ρ_N = 4, where N_{cell} for 2 gap junctions per side was lower by 1. N_{cell} was least when only 1 gap junction was present on each side. In summary, as ρ_N increased, N_{cell}, also increased. In addition, as the number of gap junctions per side was raised, N_{cell} increased.

When σ_{gap} = 0.3 (Figure 6B), as the number of gap junctions per side increased, N_{cell}, the number of cells at the decreased $\rho_A low$ of 0.05 needed for spreading depolarizations also increased. N_{cell} values were greatest when there was only 1 gap junction connection on each side. However, when ρ_N = 5, there were no values of N_{cell} at which spreading depolarizations occurred. When there were 2 and 3 gap junctions per side, N_{cell} values were decreased by one, compared to when there was 1 gap junction per side, at every value of ρ_N except 5. Where there were 4 and 5 gap junctions per side, N_{cell} values were the same or decreased by one, compared to when there were 2 or 3 gap junctions per cell, at all values of ρ_N. In general, when σ_{gap} = 0.3,

the number of cells set at $\rho_A low$ necessary for spreading depolarizations, N_{cell}, very slightly decreased as the number of gap junctions per side increased, N_{cell} generally decreased. For every increase of 1 in ρ_N, N_{cell} also increased by 3 to 4.

The results for when σ_{gap} = 0.5 (Figure 6C) are very similar to those when σ_{gap} = 0.3 (Figure 6B): N_{cell} slightly decreased as the number of gap junctions per side increased. As when σ_{gap} = 0.3, N_{cell} values were greatest when there was only 1 gap junction connection on each side. At 2 gap junctions per side, N_{cell} values were the same as those at 1 gap junction per side at ρ_N = 2, 4 and 5; at ρ_N = 1 and 3, N_{cell} at 2 gap junctions/side was 1 less than N_{cell} at 1 gap junction/side. At 3, 4 and 5 gap junctions, N_{cell} values were the same as those of 2 gap junctions/side at ρ_N = 1, 3 and 5. At ρ_N = 2 and 4, N_{cell} values for 3, 4 and 5 gap junctions were 1 less than those for 2 gap junctions per side. Additionally, as ρ_N increased by 1, N_{cell} also increased by 2-4.

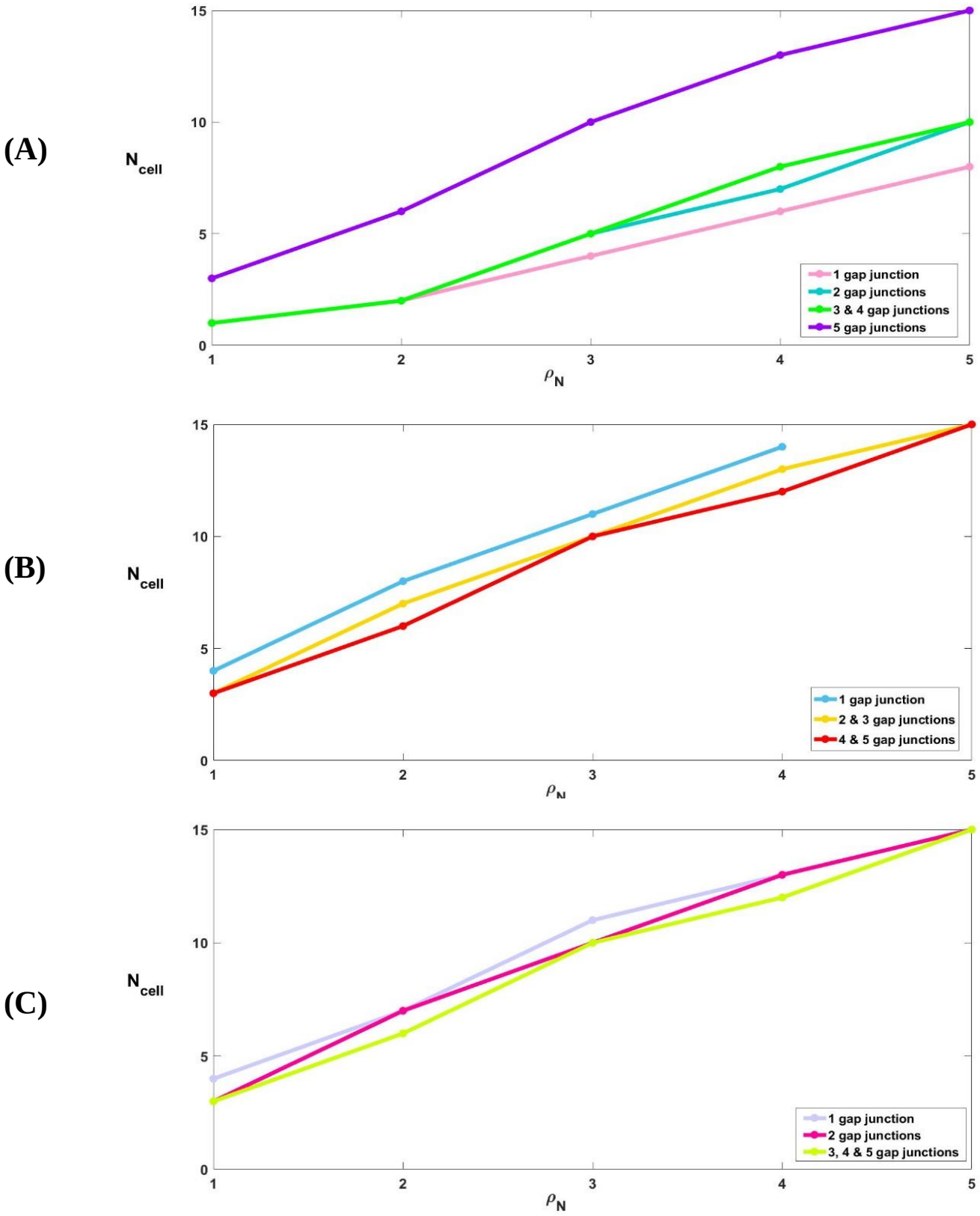

Figure 6: Dependence of N_{cell} needed for RSDs on ρ_N when: (A) $\boldsymbol{\sigma_{gap}}$, the strength of the gap junction, = 0.1; (B) $\boldsymbol{\sigma_{gap}}$ = 0.3; and (C) $\boldsymbol{\sigma_{gap}}$ = 0.5.

Discussion

We have created a mathematical model simulating biochemical processes to more fully understand the dynamics of the neurons and astrocytes that result in recurrent spreading depolarizations. Experimental results, like wave speed, changes in ion concentrations and changes in membrane potentials, are accurately simulated by our model. The results of our model indicate that the propagation of the depolarization is due to the increase and diffusion of K+, rather than glutamate, which is supported by experimental results (Enger 2015).

Previous modeling studies of spreading depolarizations and neuron-astrocyte interactions have included many of the same processes that we did, but have left out other important features (Kager 2002; Somjen 2008; Diekman 2013; Huguet 2016). We have considered the importance of the astrocytic Na^+-K^+ pump in initiating and propagating spreading depolarizations. Lowering the strength of the astrocytic Na^+-K^+ pump strength, without decreasing the neuron Na^+-K^+ pump strength, is sufficient to induce spreading depolarizations. As the astrocytic Na^+-K^+ pump strength is decreased further, fewer cells at this lower pump strength are necessary for waves to occur. Conversely, as the astrocytic Na^+-K^+ pump strength increases, more and more cells are needed to initiate recurrent spreading depolarizations.

Firstly, we have included a model for the glial Na^+-glutamate transporter. We have also included a more detailed model of the astrocyte, in which the astrocyte uptakes or releases glutamate and transfers Na^+ and K^+ to other astrocytes through gap junctions. Here, when the strength of the gap junction was a low 0.1, the number of gap junctions on each side of the astrocyte impacted how many cells at a lower astrocytic Na^+-K^+ pump strength were needed to start spreading depolarizations. The greater the number of gap junctions, more astrocytes were

needed, indicating that gap junctions made it more difficult for spreading depolarizations to occur.

However, the results were not the same when the strength of the gap junction was increased to 0.3 and 0.5. Unexpectedly, when more gap junctions were present, it became slightly easier for recurrent spreading depolarizations to occur, as evidenced by the relatively lower number of astrocytes, at a lower Na^+-K^+, pump strength needed. The reason for this result is not fully understood, but it supports the theory that in different situations, gap junctions my lead to cell survival or cell death (Farahani 2005). More research will need to be performed to truly understand what role glial gap junctions may play in initiating or propagating waves of depolarization.

There are multiple cellular processes that we have not considered in creating our model; we have focused solely on those necessary to attain recurrent spreading depolarizations. In the future, we would like to have more realistic and comprehensive network model. This would include changes in cell volumes, ATP metabolism within mitochondria, Ca^{2+}-dependent cell death, glutamate receptors other than the NMDA channel and additional neuron-astrocyte pairs. Lastly, I would like to further investigate under which conditions gap junctions are beneficial or harmful during ischemia.

References

American Stroke Association. "Atherosclerosis and Stroke." Atherosclerosis and Stroke. American Heart Association, Jan.-Feb. 2005.

Ankarcrona M, Dypbukt JM, Bonfoco E, Zhivotovsky B, Orrenius S, Lipton SA, Nicotera (1995). Glutamate-Induced Neuronal Death: A Succession of Necrosis or Apoptosis Depending on Mitochondrial Function Neuron, Vol. 15, 961-973.

Astrup J, Symon L, Branston, NM & Lassen NA (1977). Cortical evoked potential and extracellular K+ and H+ at critical levels of brain ischemia. Stroke 8, 51–57.

Back T, Ginsberg MD, Dietrich WD, Watson BD. Induction of spreading depression in the ischemic hemisphere following experimental middle cerebral artery occlusion: effect on infarct morphology. J Cereb Blood Flow Metab 16:202–213.

Busch E, Gyngell ML, Eis M, Hoehn-Berlage, Hossmann KA (1996). Potassium-Induced Cortical Spreading Depressions During Focal Cerebral Ischemia in Rats: Contribution to Lesion Growth Assessed by Diffusion-Weighted NMR and Biochemical Imaging. J Cereb Blood Flow Metab 16:1090-1099.

Choi DW, Rothman SM (1990). The Role of Glutamate Neurotoxicity in Hypoxic-Ischemic Neuronal Death. Annu Rev Neurosci 13:171-182.

Danbolt NC, Furness DN, Zhou Y (2016). Neuronal vs glial glutamate uptake: resolving the conundrum. Neurochem Int 98: 29-45.

Diekman CO, Fall CP, Lechleiter JD, Terman D (2013). Modeling the neuroprotective role of enhanced astrocyte mitochondrial metabolism during stroke. Biophysical Journal 104: 1752–1763.

Dirnagl U, Iadecola C, Moskowitz MA (1999). Pathobiology of ischaemic stroke: An integrated view. doi10.1016/S0166-2236(99)01401-0.

Dreier JP (2011). The role of spreading depression, spreading depolarization and spreading ischemia in neurological disease. Nat Med 17: 439–447.

Enger R, Tang W, Vindedal GF, Jensen V, Johannes Helm P, Sprengel R, Looger LL, Nagelhus EA (2015). Dynamics of Ionic Shifts in Cortical Spreading Depression. Cerebral Cortex 25: 4469-4476.

Ermentrout GB, Terman DH (2010). Mathematical foundations of neuroscience, volume 35 of nterdisciplinary Applied Mathematics. Springer, New York, xvi+422 pp.

Fall CP, Keizer J (2001). Mitochondrial modulation of intracellular Ca2+ signaling. Journal of Theoretical Biology 210:151–165.

Farahani R, Pina-Benabou M, Kyrozis A, Siddiq A, Barradas PC, Chiu FC, Cavalcante LA, Lai JCK, Stanton PK, Rozental R (2005). Alterations in Metabolism and Gap Junction Expression

May Determine the Role of Astrocytes As ‘‘Good Samaritans’’ or Executioners. Glia 50:351–361.

Hartings J, Watanabe T, Bullock MR, Okonkwo DO, Fabricius M, Johannes W, Dreier JP, Puccio A, Shutter LA, Clemens P, Strong AJ (2011). Spreading depolarizations have prolonged directcurrent shifts and are associated with pooroutcome in brain trauma. Brain 2011: 134; 1529–1540.

Higuchi T, Takeda Y, Hashimoto M., Nagano O, Hirakawa M (2002). Dynamic changes in cortical NADH fluorescence and direct current potential in rat focal ischemia: relationship between propagation of recurrent depolarization and growth of the ischemic core. J. Cereb. Blood Flow Metab. 22, 71–79.

Hille B (2001). Ion channels and excitable membranes. Sinauer Associates; 3rd Edition.

Hossmann KA (1994). Viability thresholds and the penumbra of focal ischemia. Ann Neurol 36:557–565.

Huguet G, Joglekar A, Matamba Messi L, Buckalew R, Wong S, Terman D (2016). Neuroprotective Role of Gap Junctions in a Neuron Astrocyte Network Model. Biophysical J 111: 452-462. (2016)

Iadecola C, Anrather J (2011). The immunology of stroke: from mechanisms to translation. Nat Med 7(7): 796–808.

Lauritzen, M (1994). Pathophysiology of the migraine aura. The spreading depression theory. Brain 117, 199–210.

Levy L, Warr O, Attwell D (1998). Stoichiometry of the Glial Glutamate Transporter GLT-1 Expressed Inducibly in a Chinese Hamster Ovary Cell Line Selected for Low Endogenous Na1-Dependent Glutamate Uptake. J. Neurosci 18(23):9620–9628.

Li YX, Rinzel J (1994). Equations for InsP3 receptor-mediated $[Ca2^{+}]_i$ oscillations derived from a detailed kinetic model: a Hodgkin-Huxley like formalism. Journal of Theoretical Biology 166: 461–473.

Lipton P (1999). Ischemic cell death in brain neurons. Physiol Rev 79(4): 1431–1568.

Lo EH, Moskowitz MA, Jacobs TP (2005). Exciting, radical, suicidal: how brain cells die after stroke. Stroke 36(2): 189-92.

Lo EH (2008). A new penumbra: transitioning from injury into repair after stroke. Nat Med 14(5):497-500.

Moskowitz MA, Lo EH, Iadecola C (2011). The Science of Stroke: Mechanisms in Search of Treatments. Neuron Review 67: 181-198.

Mozaffarian D, Benjamin EJ, Go AS, Arnett DK, Blaha MJ, et al. (2015). Heart disease and stroke statistics—2015 update: a report from the American Heart Association. Circulation 131(4):e29–322.

Nakamura H, Strong AJ, Dohmen C, Sakowitz OW, Vollmar S, Sue M, Kracht L, Hashemi P, Bhatia R, Yoshimine T, Dreier J, Dunn AK, Graf R (2010). Spreading depolarizations cycle around and enlarge focal ischaemic brain lesions. Brain: 133; 1994–2006

National Center for Chronic Disease Prevention and Health Promotion, Division for Heart Disease and Stroke Prevention (2016). Stroke Facts. Centers for Disease Control and Prevention. Centers for Disease Control and Prevention.

National Institutes of Health (2004). What You Need to Know About Stroke." National Institutes of Health. U.S. Department of Health and Human Services.

National Institute of Neurological Disorders and Stroke (2004). Stroke: Hope Through Research. National Institutes of Health, U.S. Department of Health and Human Services.

Phillis JW, Smith-Barbour M, O'Regan MH (1996). Changes in extracellular amino acid neurotransmitters and purines during and following ischemias of different durations in the rat cerebral cortex. Neurochem. Int. 29, 115–120.

Pietrobon D, Moskowitz M (2014). Chaos and commotion in the wake of cortical spreading depression and spreading depolarizations. Nature Reviews Neuroscience 15: 379–93.

Risher WC, Ard D, Yuan J, Kirov SA (2010). Recurrent spontaneous spreading depolarizations facilitate acute dendritic injury in the ischemic penumbra. The Journal of Neuroscience: the official journal of the Society for Neuroscience 30: 9859–9868.

Rossi DJ, Oshima T, Attwell D (2000). Glutamate release in severe brain ischaemia is mainly by reversed uptake. Nature 403, 316–321.

Rossi DJ, Brady JD, Mohr C (2007). Astrocyte metabolism and signaling during brain ischemia. Nature Neuroscience 10: 1377-1386.

Shin HK, Dunn AK, Jones PB, Boas DA, Moskowitz MA, Ayata C (2005). Vasoconstrictive neurovascular coupling during focal ischemic depolarizations. J Cereb Blood Flow Metab 26: 1018–30.

Somjen GG (2001) Mechanisms of spreading depression and hypoxic spreading depression-like depolarization. Physiological Reviews 81: 1065–1096.

Somjen GG, Kager H, Wadman WJ (2008) Computer simulations of neuron-glia interactions mediated by ion flux. Journal of Computational Neuroscience 25: 349–365.

Szatkowski, M, Attwell, D (1994). Triggering and execution of neuronal death in brain ischaemia: two phases of glutamate release by different mechanisms. Trends Neurosci. 17, 359–365.

Xing C, Arai K, Lo EH, Hommel M (2012). Pathophysiologic cascades in ischemic stroke. Int J Stroke 7(5): 378–385.